Письма в ЭЧАЯ. 2010. Т. 7, № 2(158). С. 128–141

SANCNEWS: TOP DECAYS IN QCD AND EW SECTORS

D. Bardin [a], *S. Bondarenko* [a], *P. Christova* [a],
L. Kalinovskaya [a], *V. Kolesnikov* [a], *W. von Schlippe* [b]

[a] Joint Institute for Nuclear Research, Dubna
[b] St. Petersburg Nuclear Physics Institute, St. Petersburg, Russia

In this paper we present the results of the implementation of the decay $t \to b\, f_1 \bar{f}_1'$ into the SANC system (f_1 is a massless fermion). The new aspect of the work is the combination of QCD and EW corrections. All calculations are done at the one-loop level in the Standard Model. We give a detailed account of the new procedure — the forming of a class of $J_{AW,WA}$ functions. These functions are related to the procedure of extraction of infrared and mass-shell singular divergences. The emphasis of this paper is on the presentation of numerical results for various approaches: complete one-loop calculations and different versions of pole approximations.

Представлена реализация распадов $t \to b\, f_1 \bar{f}_1'$ в рамках системы SANC (f_1 обозначает безмассовый фермион). Впервые демонстрируется комбинация КХД- и электрослабых (ЭС) поправок. Все расчеты выполнены в однопетлевом приближении Стандартной модели. Детально рассмотрена новая процедура SANC — формирование класса $J_{AW,WA}$-функций. Данные функции связаны с процедурой извлечения инфракрасных расходимостей и массовых сингулярностей. Представлены численные результаты различных подходов: полных однопетлевых поправок и различных версий полюсного приближения.

PACS: 12.15.Lk, 13.40.Ks, 14.65.Ha

INTRODUCTION

In this paper we review the state-of-art of the implementation of NLO QCD and electroweak (EW) radiative corrections (RC) to the charge current decays

$$F \to f f_1 \bar{f}_1'(\gamma, g) \tag{1}$$

(where F and f denote massive fermions and f_1 and f_1' denote massless fermions) within the framework of the SANC system [1, 2].

This work is a continuation of our previous one [3], devoted to the EW Radiative Corrections (EWRC) to $t \to bl^+\nu_l$ decay. Here we extend it in two directions: addition of quark channels, e.g., $t \to bu\bar{d}$, etc., and of the NLO QCD corrections, see also [4] and references therein. The implementation of QCD corrections into SANC for some 3- and 4-leg processes is presented in [5].

Recall that in SANC we always calculate any one-loop process amplitude as annihilation into vacuum with all 4-momenta incoming. Therefore, the derived form factors for the amplitude of the process $tb\bar{u}\bar{d} \to 0$ after an appropriate permutation of their arguments may

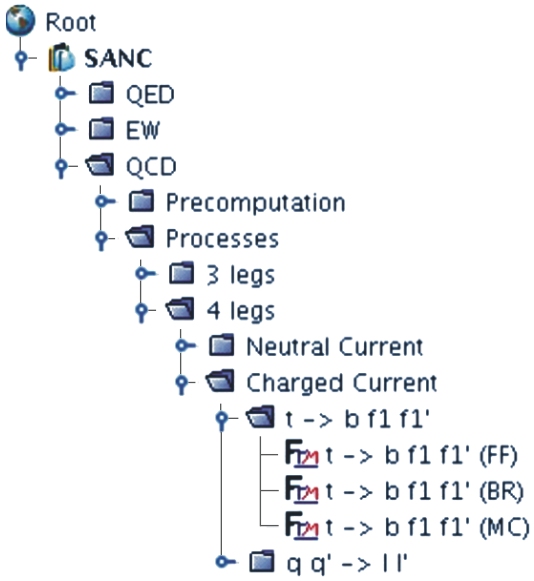

Fig. 1. QCD node: $t \to bf_1\bar{f}_1'$

be used for the description of NLO corrections of the single top production processes, e.g., s-channel $ud \to tb$, and t-channel $ub \to dt$.

The QCD tree for the $t \to bf_1\bar{f}_1'$ processes is shown in Fig. 1.

A similar tree was already shown in the previous paper [3] for the EW branch. Nowadays, within SANC we follow the strategy to present both EW and QCD NLO RC simultaneously, realizing them as the SSFM (Standard SANC (FORM/FORTRAN) Modules). We use FORM version 3.1 [6]. The modules are united into two packages (CC and NC). The concept of modules is decribed in [7], ibidem the previous versions 1.20, see also [8].

The packages are reachable for users from our project homepages [9]. Both EW and QCD RC modules of these processes $t \to bf_1\bar{f}_1'$ will be put into version 1.30 of the CC package.

A first attempt to combine QCD and EW corrections within the SANC project was done for DY CC processes and presented in talks at the ATLAS MC Working Group [10] and later on in the paper [11].

This paper is devoted to the complete NLO QCD and EW radiative corrections to the 4-leg top quark decays $t \to bf_1\bar{f}_1'(\gamma, g)$. We also discuss how the SANC results of complete one-loop calculations are compared with the results of various approximate cascade approaches.

These exercises are necessary in order to make the right choice in the future: how we would sew together NLO 4-leg and 3-leg building blocks, available in SANC [1]. For example, 4-leg and 3-leg blocks in the description of a cascade of the type $f_1\bar{f}_1 \to HZ; Z \to \mu^+\mu^-$ or two 4-leg blocks in $ud \to bt; t \to bl\nu$; the results of these studies will be published elsewhere.

This paper is organized as follows. In Sec. 1 we review the complete calculations as adopted within the SANC framework. The standard narrow width cascade approach, that with a complex W boson mass, and the cascade in the pole approximation with a finite W width

are presented in Sec. 2. Numerical results are collected in Sec. 3. Finally, at the end of the paper we present our conclusions.

1. COMPLETE EWRC

1.1. The Separation of QED Corrections. The complete one-loop EW corrections for $t(p_2) \to b(p_1) + u(p_3) + \bar{d}(p_4)$ decay are calculated by the SANC system as described in Subsec. 2.5 of [1]. The covariant amplitudes $\mathcal{A}$ and helicity amplitudes $\mathcal{H}_{ijkl}$ are given by Eqs. (43)–(46) with $D_\mu = -(p_1+p_2)_\mu$ and Eqs. (47)–(50), respectively. They are expressed in terms of four scalar form factors: $\mathcal{F}_{LL}$, $\mathcal{F}_{RL}$, $\mathcal{F}_{LD}$, $\mathcal{F}_{RD}$. It is useful to extract the QED part from the complete EW amplitude. Only the LL form factor contains both QED and weak contributions:

$$\mathcal{F}_{LL} = 1 + \frac{e^2}{16\pi^2}\widetilde{\mathcal{F}}_{LL}^{\rm QED} + \frac{g^2}{16\pi^2}\widetilde{\mathcal{F}}_{LL}^{\rm weak}. \tag{2}$$

The other three form factors contain only weak parts. There exists no gauge-invariant separation of the QED part from the entire LL form factor. We choose it in the simplest and most natural form:

$$\begin{aligned}
\widetilde{\mathcal{F}}_{LL}^{\rm QED} = 2\Big[&-Q_uQ_dQ^2C_0(-m_u^2,-m_d^2,Q^2;m_u,\lambda,m_d) - Q_uQ_t(T^2+\\
&+m_t^2)C_0(-m_u^2,-m_t^2,T^2;m_u,\lambda,m_t) + Q_uQ_bU^2C_0(-m_u^2,-m_b^2,U^2;m_u,\lambda,m_b)+\\
&+Q_dQ_t(U^2+m_t^2)C_0(-m_d^2,-m_t^2,U^2;m_d,\lambda,m_t)-\\
&-Q_dQ_bT^2C_0(-m_d^2,-m_b^2,T^2;m_d,\lambda,m_b)-Q_tQ_b(Q^2+m_t^2)C_0(-m_t^2,-m_b^2,Q^2;m_t,\lambda,m_b)\Big]-\\
&-\frac{3}{2}\Big[Q_u^2a_0^f(m_u)+Q_d^2a_0^f(m_d)+Q_t^2a_0^f(m_t)+Q_b^2a_0^f(m_b)\Big]+\\
&+Q_u^2\ln_\lambda(m_u^2)+Q_d^2\ln_\lambda(m_d^2)+Q_t^2\ln_\lambda(m_t^2)+Q_b^2\ln_\lambda(m_b^2),
\end{aligned} \tag{3}$$

with C_0 being the standard Passarino–Veltman (PV) function [12, 13] and

$$a_0^f(m) = \ln\left(\frac{m^2}{\mu^2}\right) - 1, \quad \ln_\lambda(m^2) = \ln\left(\frac{m^2}{\lambda^2}\right), \tag{4}$$

where μ is the 't Hooft (renormalization) scale and λ is a photon mass. The natural choice is $\mu = M_W$. Furthermore, in Eq. (3) we use the standard SANC definitions: $Q_f = 2I_f^3$ with I_f^3 being the weak isospin and

$$Q^2 = (p_1+p_2)^2, \qquad T^2 = (p_2+p_3)^2, \qquad U^2 = (p_2+p_4)^2, \tag{5}$$

with momenta p_i being defined in Fig. 2.

The form factor $\widetilde{\mathcal{F}}_{LL}^{\rm QED}$, as defined by Eq. (3), contains all IR divergences in four $\ln_\lambda(m^2)$ functions, one for each photon emission from an external line, and in six C_0 functions, one for each photon radiation interference term. Moreover, all logarithmic mass singularities should

be concentrated in the QED part and all weak contributions must not contain logarithmic mass singularities even at the amplitude level, having nothing to do with Kinoshita–Lee–Nauenberg (KLN) theorem. Furthermore, the gauge non-invariance of the QED/weak separation is made manifest by the presence of the 't Hooft scale. We prefer to keep terms with $a_0^f(m)$ in the QED contribution since they are mass singular.

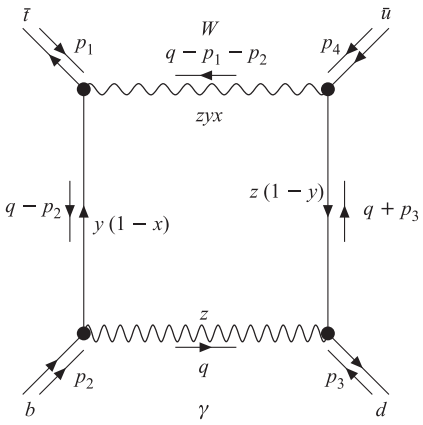

Fig. 2. Example of a $J^d_{WA}(Q^2,T^2;b,\bar{t},d,\bar{u},W)$ function

1.2. Auxiliary Functions $J_{AW,WA}$. To calculate the weak part of the RC we introduce the set of auxiliary functions $J^{d,c}_{WA,AW}$ related to «direct» and «cross» WA and AW box diagrams of the kind shown in Fig. 2. They are deeply connected to the procedure of separation of infrared and mass singularities from PV D_0 functions in terms of simplest objects — the C_0 functions. The eventually «subtracted» auxiliary functions $J_{\rm sub}$ do not contain any singularities and are expressed as linear combinations of dilogarithms, see [14]. By introducing these functions we prove, first of all, that the EW part of the one-loop correction is free from mass singularities and, moreover, receives a good profit in the stability and speed of numerical calculations. Furthermore, the explicit expressions for these functions are used for the study of «on-shell-W-mass» singularities, introduced and discussed in [15].

The letters u, $d,\ldots$ in the figure caption denote particle masses. The ordering of masses in the argument of J^d_{WA} into two pairs of heavy (b,t) and light (d,u) quarks is such that the first mass in each pair corresponds to the fermion coupled to the photon, thereby leading to the appearance of a potentially mass singular logarithmic contribution.

The basic definition of the function J^d_{WA} reads

$$i\pi^2 J^d_{WA}(Q^2,T^2;b,\bar{t},d,\bar{u},W)=\mu^{4-n}\int d^nq\frac{2q\cdot p_1}{d_0\,d_1\,d_2\,d_3},$$

where

$$\begin{aligned} &d_0=(q-p_1-p_2)^2+M_W^2,\quad d_1\;=\;(q-p_2)^2+m_b^2,\\ &d_2=q^2,\quad d_3\;=\;(q+p_3)^2+m_d^2. \end{aligned}\tag{6}$$

For t and $\bar{t}$ decays one finds eight functions, four direct and four crossed ones. The four direct ones come in two pairs (Figs. 3 and 4).

The crossed functions may be obtained by a simple permutation of their arguments.

There are four symmetry relations between direct $J^d_{AW,WA}$ and cross $J^c_{AW,WA}$ functions:

$$\begin{aligned} J^d_{AW}(Q^2,T^2;\bar{b},t,\bar{d},u,W)&=J^d_{WA}(Q^2,T^2;b,\bar{t},d,\bar{u},W),\\ J^d_{WA}(Q^2,T^2;t,\bar{b},u,\bar{d},W)&=J^d_{AW}(Q^2,T^2;\bar{t},b,\bar{u},d,W),\\ J^c_{AW}(Q^2,U^2;\bar{b},t,u,\bar{d},W)&=J^c_{WA}(Q^2,U^2;b,\bar{t},\bar{u},d,W),\\ J^c_{WA}(Q^2,U^2;t,\bar{b},\bar{d},u,W)&=J^c_{AW}(Q^2,U^2;\bar{t},b,d,\bar{u},W). \end{aligned}$$

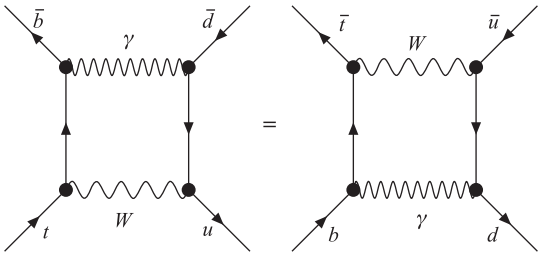

Fig. 3. First pair of direct J^d_{AW} and J^d_{WA} functions

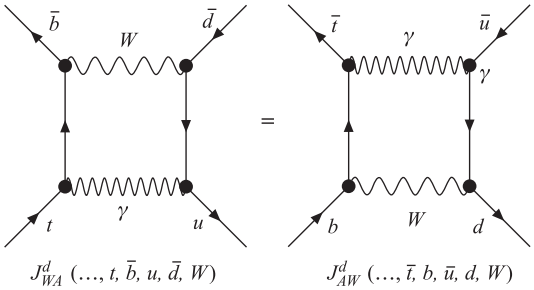

Fig. 4. Second pair of direct J^d_{WA} and J^d_{AW} functions

So, only four functions are independent. Moreover, as seen from the previous relations, the indices content of the $J^d_{AW}\ldots$ functions (retained for better understanding of their origin from corresponding Feynman diagrams) is uniquely determined by their arguments. Therefore, these indices may be dropped in the subsequent presentation of the material. Also, the particle names will be changed to particle masses in the arguments of these functions.

1.2.1. Steps to Calculate J Functions

• *Step: relations for J.* Using the standard PV reduction it is possible to establish relations (exact in masses) between infrared divergent functions (from here and below, we use the usual notation for particle masses):

$$D_0(-m_b^2,-m_t^2,-m_u^2,-m_d^2,Q^2,T^2;0,m_b,M_W,m_d),\quad C_0(-m_d^2,-m_b^2,T^2;m_d,0,m_b)$$

and infrared finite, but mass-singular functions:

$$J(Q^2,T^2;m_b,m_t,m_d,m_u,M_W)\quad\text{and}\quad C_0(-m_u^2,-m_d^2,Q^2;M_W,m_d,0).$$

For direct functions these relations are

$$\begin{aligned}J(Q^2,T^2;m_b,m_t,m_d,m_u,M_W)&=\\ &=(M_W^2+Q^2)D_0(-m_b^2,-m_t^2,-m_u^2,-m_d^2,Q^2,T^2;0,m_b,M_W,m_d)+\\ &\quad+C_0(-m_u^2,-m_d^2,Q^2;M_W,m_d,0)-C_0(-m_d^2,-m_b^2,T^2;m_d,0,m_b),\end{aligned}\quad(7)$$

$$J(Q^2,T^2;m_t,m_b,m_u,m_d,M_W) =$$
$$= (M_W^2+Q^2)D_0(-m_b^2,-m_t^2,-m_u^2,-m_d^2,Q^2,T^2;M_W,m_t,0,m_u)+$$
$$+ C_0(-m_u^2,-m_d^2,Q^2;0,m_u,M_W) - C_0(-m_t^2,-m_u^2,T^2;m_t,0,m_u). \quad (8)$$

For the crossed functions we perform the appropriate permutations of the arguments of these functions.

Then, we calculate the functions J exactly in masses in terms of dilogarithms. Finally, we take the limit $m_u, m_d \to 0$, neglecting light quark masses everywhere but mass singular logarithms. These two steps represent rather complicated procedures, which will be described elsewhere [16].

• *Step:* $J_{\rm sub}$. The mass singularities in arguments of the logarithms may be compensated by combination with one more C_0 function:

$$J_{\rm sub}(Q^2,P^2;m_b,m_t,M_W) = J(Q^2,P^2;m_b,m_t,m_d,m_u,M_W)-$$
$$- \left(1+\frac{Q^2}{m_b^2+P^2}\right) C_0(-m_u^2,-m_d^2,Q^2;M_W,m_d,0),$$
$$J_{\rm sub}(Q^2,P^2;m_t,m_b,M_W) = J(Q^2,P^2;m_t,m_b,m_u,m_d,M_W)-$$
$$- \left(1+\frac{Q^2}{m_t^2+P^2}\right) C_0(-m_d^2,-m_u^2,Q^2;M_W,m_u,0),$$

where $P^2 = T^2$ or $P^2 = U^2$. The two mass singular C_0 functions appearing in Eq. (9) cancel in the total expression for the EW correction which proves the absence in it of logarithmic mass singularities (not KLN theorem!).

• *Step:* $J_{\rm subsub}$. If we want to neglect the m_b mass, we should perform the second subtraction of a mass singular C_0 function $C_0(-m_t^2,-m_b^2,Q^2,M_W,m_b,0)$ that appears in the limit $m_b = 0$.

Note that only one of $J_{\rm sub}$ contains an m_b mass singularity.

$$J_{\rm subsub}(Q^2,P^2;m_b,m_t,M_W) = J_{\rm sub}(Q^2,P^2;m_b,m_t,M_W)-$$
$$- \frac{P^2}{Q^2+m_t^2} C_0(-m_t^2,-m_b^2,Q^2;M_W,m_b,0). \quad (9)$$

Since we do not want to consider the limit $m_t = 0$, we simply rename the second function:

$$J_{\rm subsub}(Q^2,P^2;m_t,m_b,M_W) = J_{\rm sub}(Q^2,P^2;m_t,m_b,M_W). \quad (10)$$

Again, the m_b mass singular C_0 function $C_0(-m_t^2,-m_b^2,Q^2;M_W,m_b,0)$ cancels in the total EW correction.

1.2.2. Treatment of On-Shell-W-Mass Singularities. In the course of calculations of the $\mathcal{O}(\alpha)$ EWRC one encounters *on-shell* singularities which appear in the form of $\ln(s-M_W^2+i\epsilon)$. We follow [15] where it was shown that they can be regularized by the W width:

$$\ln(s-M_W^2+i\epsilon) \to \ln(s-M_W^2+iM_W\Gamma_W). \quad (11)$$

Note that the replacement $M_W^2 - i\epsilon \to M_W^2 - iM_W\Gamma_W$ should be done only in the argument of logarithms which diverge at the resonance $s = M_W^2$. In this connection we derived for all $J_{\rm subsub}$ functions such a representation in which these divergent logarithms appear only once and Γ_W propagates only in it. Everywhere else we retain $M_W^2 - i\epsilon$. The explicit formulae for $J_{\rm subsub}$ functions will be presented elsewhere [16].

We also meet the on-shell singular C_0 and B_0 functions. They correspond to non-Abelian Wff' vertex functions with a virtual photon coupled to one of the fermions of mass m and to a W boson and to the W-boson self-energy diagram, respectively. We give explicit expressions for both functions:

$$\begin{aligned} C_0(0,-m^2,-s;M_W,m,0) = \\ = \frac{1}{m^2-s}\left[\ln\left(\frac{s}{m^2}\right)\ln\left(-\frac{s-M_W^2+iM_W\Gamma_W}{m^2-M_W^2}\right) - \frac{1}{2}\ln^2\left(\frac{s}{m^2}\right) - \right. \\ \left. - \mathrm{Li}_2\left(\frac{m^2(-s+M_W^2-i\epsilon)}{s(M_W^2-m^2)}\right) - \mathrm{Li}_2\left(\frac{s}{m^2-i\epsilon}\right) + \mathrm{Li}_2\left(\frac{-s+M_W^2-i\epsilon}{M_W^2-m^2}\right) + \mathrm{Li}_2(1)\right], \end{aligned} \tag{12}$$

where the first «0» stands for a fermion whose mass may be ignored (neutrino or b quark); and

$$B_0^F(-s,\mu^2;M_W,0) = 2 - \ln\left(\frac{M_W^2}{\mu^2}\right) - \left(1-\frac{M_W^2}{s}\right)\ln\left(-\frac{s-M_W^2+iM_W\Gamma_W}{M_W^2}\right). \tag{13}$$

2. CASCADE APPROXIMATIONS

2.1. The Usual Narrow Width Cascade. In this approach we create a narrow width cascade using one-loop $t \to Wb$ and $W \to l\nu$ formulae, i.e.,

$$\Gamma_{t\to bl\nu} = \frac{\Gamma^{\rm 1loop}_{t\to Wb}\Gamma^{\rm 1loop}_{W\to l\nu}}{\Gamma_W}. \tag{14}$$

At one loop, it is more consistent to use instead its «linearized» version

$$\Gamma_{t\to bl\nu} = \frac{\Gamma^{\rm Born}_{t\to Wb}\Gamma^{\rm Born}_{W\to l\nu}}{\Gamma_W}\left(1+\delta^{\rm 1loop}_{t\to Wb}+\delta^{\rm 1loop}_{W\to l\nu}\right), \tag{15}$$

where $\delta^{\rm 1loop} = \Gamma^{\rm 1loop}/\Gamma^{\rm Born} - 1$.

2.2. Cascade with Complex W Mass. Another approach to the one-loop cascade approximation uses the same Eq. (14) but with a complex W mass,

$$\widetilde{M}_W^2 = M_W^2 - iM_W\Gamma_W, \tag{16}$$

in all W-boson propagators in the diagrams with radiation of real or virtual photons. This trick regularizes the corresponding infrared divergences. The modified PV functions are listed below in this section and the results of new calculations are discussed in Sec. 3.

This modification affects all infrared divergent loop and bremsstrahlung diagrams where a photon is coupled to the W boson: they all become infrared finite.

The modification of the calculation is trivial for squares and interferences of the corresponding bremsstrahlung diagrams, which after the replacement $M_W^2 \to \widetilde{M}_W^2$ may be treated like infrared stable hard photon contributions. For loop diagrams one should replace infrared divergent PV functions in expressions regularized by Γ_W. They are listed below.

2.2.1. Analytic Expression for Modified PV Functions. The infrared divergent derivative $B_0'(-M_W^2;0,\widetilde{M}_W) = [dB_0(p^2;0,\widetilde{M}_W)/dp^2]_{|p^2=-M_W^2}$ of the B_0 function, which arises from a counterterm related to the W-boson self-energy diagram, becomes

$$B_0'(-M_W^2;0,\widetilde{M}_W) = \frac{1}{M_W^2}\left[1+\ln\left(\frac{\widetilde{M}_W^2-M_W^2}{M_W^2}\right)\right]. \tag{17}$$

There is only one generic C_0 3-point function with a photon coupled to the W boson and a fermion with mass m_2; m_1 is the mass of the other fermion:

$$C_0(-m_1^2,-m_2^2,-M_W^2;\widetilde{M}_W,m_2,0) = \frac{1}{S_l}\left\{\left[-\ln\left(\frac{\widetilde{M}_W^2-M_W^2}{m_2^2}\right)l\left(y_{l_1}\right)+\frac{1}{2}l^2\left(y_{l_1}\right)+\right.\right.$$
$$\left.\left.+\ln\left(1-\frac{y_{l_1}}{y_{l_2}}\right)l\left(y_{l_1}\right)-\mathrm{Li}_2\left(\frac{1-y_{l_1}}{y_{l_2}-y_{l_1}}\right)+\mathrm{Li}_2\left(\frac{-y_{l_1}}{y_{l_2}-y_{l_1}}\right)-\mathrm{Li}_2\left(\frac{1}{y_{l_1}}\right)\right]-\left[y_{l_1}\leftrightarrow y_{l_2}\right]\right\}. \tag{18}$$

Here

$$l(y) = \ln\left(1-\frac{1}{y}\right) \tag{19}$$

and

$$y_{l_1} = \frac{m_1^2+m_2^2-M_W^2+i\epsilon+S_l}{2m_1^2}, \quad y_{l_2} = \frac{m_1^2+m_2^2-M_W^2+i\epsilon-S_l}{2m_1^2},$$
$$S_l = \sqrt{(m_1^2+m_2^2-M_W^2+i\epsilon)^2-4m_1^2m_2^2}. \tag{20}$$

Its limit, where the radiating mass m_2 is arbitrary and the other fermion mass is zero, is much more compact:

$$C_0(0,-m_2^2,Q^2;\widetilde{M}_W,m_2,0) = \frac{1}{M_W^2-m_2^2}\left[-\ln\left(\frac{\widetilde{M}_W^2-M_W^2}{m_2^2}\right)l\left(y_l\right)+\frac{1}{2}l^2\left(y_l\right)-\mathrm{Li}_2\left(\frac{1}{y_l}\right)\right], \tag{21}$$

where

$$y_l = \frac{m_2^2}{m_2^2-M_W^2+i\epsilon}. \tag{22}$$

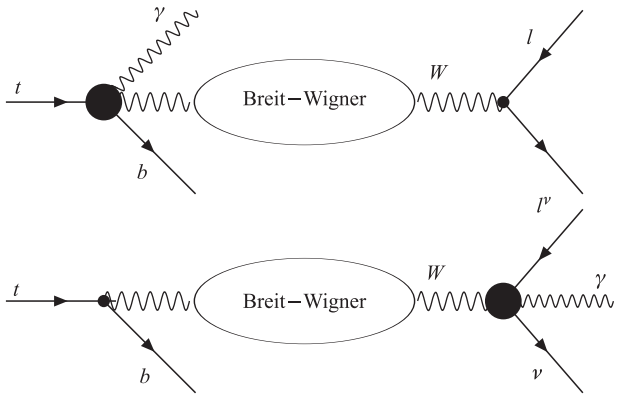

Fig. 5. $t \to bf_1f_1$ decay

Finally, in the limit $m_2 \to 0$, Eq. (18) simplifies to

$$C_0(-m_1^2,-m_2^2,-M_w^2;\widetilde{M}_w,m_2,0) = \frac{1}{m_1^2-M_w^2}\left[-\ln\left(\frac{m_2^2}{m_1^2}\right)\ln\left(\frac{\widetilde{M}_w^2-M_w^2}{m_1^2-M_w^2}\right)+\right.$$
$$+\ln\left(\frac{\widetilde{M}_w^2-M_w^2}{m_1^2}\right)\left[2\ln(-y_l)-\ln(1-y_l)\right]+$$
$$\left.+\frac{1}{2}\ln^2(1-y_l)-2\ln^2(-y_l)-\mathrm{Li}_2(y_l)-2\mathrm{Li}_2(1)\right], \quad (23)$$

where

$$y_l = \frac{m_1^2-M_w^2+i\epsilon}{m_1^2}. \quad (24)$$

In Eq. (23) the mass singular term is separated out explicitly. This expression is especially convenient if one wants to control mass singularities.

2.3. Pole Approximation. Here we present the cascade pole approximation with the aid of the two one-loop building blocks as illustrated in Fig. 5. This gives a schematic representation of a convolution of a Breit–Wigner distribution for a virtual W boson with two pairs of building blocks: one at one-loop level (big blob) and the second one at tree level, and vice versa.

First, define the one-loop corrected decay width for two decays *off the W mass shell at some $\hat{M}_w^2$*:

$$\Gamma^{1\mathrm{loop}}_{t\to Wb}(\hat{M}_w^2) = \Gamma^{\mathrm{Born}}_{t\to Wb}(\hat{M}_w^2)\left[1+\delta^{\mathrm{weak}}_{t\to Wb}(M_w^2)\right]+\Gamma^{\mathrm{virtsoft}}_{t\to Wb}(\hat{M}_w^2)+\Gamma^{\mathrm{hard}}_{t\to Wb}(\hat{M}_w^2) \quad (25)$$

and a similar representation for the $W \to l\nu$ decay.

Note that δ^{weak} is frozen at M_w^2. This trick ensures an approximate gauge invariance for CC processes (for NC processes it would ensure exact gauge invariance).

The one-loop $\Gamma^{1\mathrm{loop}}_{t\to bl\nu}$ is given by the following convolution integral:

$$\Gamma^{1\mathrm{loop}}_{t\to bl\nu} = \frac{1}{k}\int\limits_{l}^{u} d\hat{M}_W^2 \Big[\Gamma^{1\mathrm{loop}}_{t\to Wb}(\hat{M}_W^2)\Gamma^{\mathrm{Born}}_{W\to l\nu}(\hat{M}_W^2)+$$

$$+\,\Gamma^{1\mathrm{loop}}_{W\to l\nu}(\hat{M}_W^2)\Gamma^{\mathrm{Born}}_{t\to Wb}(\hat{M}_W^2) - \Gamma^{\mathrm{Born}}_{t\to Wb}(\hat{M}_W^2)\Gamma^{\mathrm{Born}}_{W\to l\nu}(\hat{M}_W^2)\Big]\frac{M_W}{(\hat{M}_W^2-M_W^2)^2+M_W^2\Gamma_W^2}, \quad (26)$$

where k is given by the normalization of the Breit–Wigner distribution and u and l are the broadest limits allowed by the decay kinematics:

$$k = a\tan(k_{\min}) + a\tan(k_{\max}), \quad u = M_W^2 + k_{\max}M_W\Gamma_W, \quad l = M_W^2 - k_{\min}M_W\Gamma_W,$$
$$k_{\min} = \frac{M_W^2-m_l^2}{M_W\Gamma_W}, \quad k_{\max} = \frac{(m_t-m_b)^2-M_W^2}{M_W\Gamma_W}, \quad (27)$$

where m_l is the charged lepton mass.

This *finite width approximation*, as one may call it, allows a fully differential realization, and hence also MC generation.

3. NUMERICAL RESULTS

We present all numbers, computed with the standard `SANC INPUT`, PDG(2006) [17]:

$$\begin{aligned}
G_F &= 1.16637\cdot 10^{-5}\,\mathrm{GeV}^{-2}, & \alpha(0) &= 1/137.03599911,\\
M_W &= 80.403\ \mathrm{GeV}, & \Gamma_W &= 2.141\ \mathrm{GeV},\\
M_Z &= 91.1876\ \mathrm{GeV}, & M_H &= 120\ \mathrm{GeV},\\
m_e &= 0.51099892\,\mathrm{MeV}, & m_u &= 62\ \mathrm{MeV},\\
m_d &= 83\ \mathrm{MeV}, & m_\tau &= 1.77699\ \mathrm{GeV},\\
m_c &= 1.5\ \mathrm{GeV}, & m_s &= 215\ \mathrm{MeV},\\
m_b &= 4.7\ \mathrm{GeV}, & m_t &= 174.2\ \mathrm{GeV},\\
m_\mu &= 0.105658369\,\mathrm{GeV}, & \alpha_s &= 0.107.
\end{aligned}$$

First, we investigate the dependence of the complete one-loop EW results on the b-quark mass, m_b, since the formulas with finite mass are very cumbersome. The calculations are performed for two decay channels and two schemes: with and without taking account of Γ_W to regularize on-shell W-boson singularities as discussed in Subsubsec. 1.2.2. Table 3 shows QCD NLO results, where the account of Γ_W is irrelevant since the gluons are not coupled to the W boson.

As seen from Tables 1–3, EW and QCD corrections have the opposite sign and QCD corrections are relatively larger. The m_b dependence is barely visible in $\Gamma^{1\mathrm{loop}}$ and consistent with no-dependence in δ within the statistical errors. This allows us to simplify the analysis and to present all the subsequent results at a small m_b using simplified formulae for weak one-loop contributions for $m_b = 0$. The QED/QCD contributions contain $\ln(m_b)$ in different

Table 1. **One-loop decay widths $\Gamma^{1\mathrm{loop}}$ and percentage of the EWRC for complete calculations in $\alpha(0)$-scheme as a function of the m_b mass and with Γ_W kept only in on-shell W-boson singular terms**

m_b,	$t \to bl^+\bar{\nu}_l$		$t \to bu\bar{d}$	
GeV	$\Gamma^{1\mathrm{loop}}$, MeV	$\delta, \%$	$\Gamma^{1\mathrm{loop}}$, MeV	$\delta, \%$
4.7	159.874(1)	6.951(1)	480.338(3)	7.111(1)
1.0	159.873(1)	6.951(1)	480.339(3)	7.111(1)
0.1	159.873(1)	6.950(1)	480.339(3)	7.111(1)

Table 2. **One-loop decay widths $\Gamma^{1\mathrm{loop}}$ and percentage of the EWRC for complete calculations in $\alpha(0)$-scheme as a function of the m_b mass and without regularization of on-shell W-boson singularities**

m_b,	$t \to bl^+\bar{\nu}_l$		$t \to bu\bar{d}$	
GeV	$\Gamma^{1\mathrm{loop}}$, MeV	$\delta, \%$	$\Gamma^{1\mathrm{loop}}$, MeV	$\delta, \%$
4.7	159.943(3)	6.997(2)	480.661(6)	7.183(1)
1.0	159.938(3)	6.993(2)	480.658(6)	7.182(1)
0.1	159.937(3)	6.993(2)	480.656(6)	7.182(1)

Table 3. **One-loop decay widths $\Gamma^{1\mathrm{loop}}$ and percentage of the QCD correction for complete calculations in $\alpha(0)$-scheme as a function of the m_b mass**

m_b,	$t \to bl^+\bar{\nu}_l$		$t \to bu\bar{d}$	
GeV	$\Gamma^{1\mathrm{loop}}$, MeV	$\delta, \%$	$\Gamma^{1\mathrm{loop}}$, MeV	$\delta, \%$
4.7	136.71(1)	–8.54(1)	358.50(17)	–20.06(4)
1.0	136.70(1)	–8.55(1)	358.52(19)	–20.05(4)
0.1	136.71(6)	–8.55(1)	358.49(22)	–20.06(5)

parts but they cancel in the sum in accordance with the KLN theorem. Tables 1–3 demonstrate the validity of the KLN theorem.

For definiteness, the numbers presented in the following Tables, after Table 3, are computed for $m_b = 1$ GeV, since even at $m_b = 4.7$ GeV the numbers are practically the same as at $m_b = 0.1$ GeV.

All numbers presented in Tables 1 and 3 may be reproduced by `SANC` package `sanc_cc_v1.30`.

In Table 4 we illustrate the Γ_W dependence of EWRC to the two channels under consideration, irrelevant for QCD NLO corrections.

This Table illustrates the perfect convergence with lowering Γ_W and consistency of numbers for $\Gamma_W/10^2$ with results computed with zero width in arguments of functions with on-shell-W-mass singularities, see Subsubsec. 1.2.2.

Table 4. **One-loop decay widths and percentage of the EWRC for complete calculations in $\alpha(0)$-scheme as a function of Γ_W**

Γ_W/N	$t \to bl^+\bar{\nu}_l$		$t \to bu\bar{d}$	
N	$\Gamma^{\rm 1loop}$, MeV	$\delta, \%$	$\Gamma^{\rm 1loop}$, MeV	$\delta, \%$
1	159.874(1)	6.951(1)	480.338(3)	7.111(1)
10	159.943(3)	6.997(2)	480.638(6)	7.177(1)
10^2	159.938(3)	6.994(2)	480.656(6)	7.182(1)
10^3	159.938(3)	6.993(2)	480.658(6)	7.182(1)
∞	159.938(3)	6.993(2)	480.658(6)	7.182(1)

Table 5. **Born, one-loop decay widths and percentage of the correction in narrow width cascade approximation, $\alpha(0)$-scheme**

	$t \to Wb$	$W \to e\nu$	$t \to be\nu$ cascade
$\Gamma^{\rm Born}$, MeV	1480.0	219.70	151.87
$\Gamma^{\rm 1loop}$, MeV	1546.6	225.28	162.73
$\delta, \%$	4.495	2.538	7.155
$\delta_{\rm lin}, \%$			7.033

Table 6. **One-loop decay widths and percentage of the correction in cascade approximation with complex W mass**

Γ_W/N	$t \to Wb$		$W \to e\nu$		$t \to bl\nu$ cascade	
N	$\Gamma_{t\to Wb}$, MeV	δ,%	$\Gamma_{W\to e\nu}$, MeV	δ,%,	$\Gamma_{t\to bl\nu}$, MeV	δ, %
1	1543.4	4.29	225.05	2.43	162.23	6.83
10	1543.0	4.26	224.79	2.32	162.00	6.68
10^2	1543.0	4.26	224.77	2.31	161.99	6.67
10^3	1543.0	4.26	224.77	2.31	161.99	6.67

Now turn to the study of narrow width cascade approaches, see Sec. 2. All numbers are presented in the $\alpha(0)$-scheme for definiteness. Here we limit ourselves to EWRC, because of the vanishing of gW boxes in the QCD case. Comparison of complete and cascade approaches shows in particular the importance of EW boxes which are absent in the cascade approach. Two δs are shown corresponding to Eq. (14), factorized version, and Eq. (15), linearized version.

Table 5 shows rather good agreement of complete and narrow width cascade calculations for inclusive quantities. The linearized version agrees better. This is natural, since the complete calculations in `SANC` are linearized by default.

Table 7. **Born, one-loop decay widths and percentage of the EWRC for the pole approximation, $\alpha(0)$-scheme, as a function of Γ_W**

Γ_W/N	$t \to bl^+\bar{\nu}_l$		
N	$\Gamma^{\rm Born}$, MeV	$\Gamma^{\rm 1loop}$, MeV	$\delta, \%$
1	153.244(1)	164.015(1)	7.029(1)
10	152.007(1)	162.696(1)	7.032(1)
10^2	151.880(1)	162.561(1)	7.032(1)
10^3	151.868(1)	162.548(1)	7.032(1)

Next, Table 6 shows the results of the cascade approach with complex W mass, see Subsec. 2.2.

There is again good convergence with decreasing Γ_W, however, we see that the agreement of this cascade version with the complete one-loop calculation (see Table 1) degrades with decreasing W-boson width.

Finally, in Table 7 we present the results of calculations within the finite width cascade approach in the pole approximation for the $t \to bl^+\bar{\nu}_l$ decay.

This is the main result of the study of the validity of resonance approaches and it deserves a detailed discussion. By now we only note that there is convergence with decreasing Γ_W and full consistency with the narrow width cascade results. Since this approach is aimed at extending the cascade approximation to the description of exclusive quantities, it is worth testing it for a simple distribution, like $d\Gamma/ds$, where s is the invariant mass squared of the $l^+\bar{\nu}_l$ pair.

CONCLUSIONS

We have described the work for the $t \to bf_1f_1'$ decays. We have computed both QCD and EW total one-loop corrections within the SANC system for all decays.

We have discussed EW corrections in more detail as they are more complicated than QCD. We have considered the problem of separating of the QED contribution from the complete EW correction.

Auxiliary functions $J^{d(c)}_{AW(WA)}$ for these decays were introduced. Then, we have presented numerical results, obtained with the aid of a Monte Carlo integrator.

We study the m_b dependence of EW and QCD corrections showing the validity of the KLN theorem. We have also demonstrated the effect of taking account of the W width in the EW contribution.

A comprehensive research of using different cascade approximations in numerical evaluations was done. The goal of this research was to check the possibility of using building blocks calculated in SANC to construct the MC tools for complicated actual processes. We have studied the narrow width cascade, cascade with complex W-mass approximations and cascade in the pole approximation. The difference between cascade methods and complete calculations shows the effect of EW boxes that are missed in the cascade approaches. However, it is

relatively small and one can see rather good agreement of cascade approaches with complete calculations. So, all these methods could be applied.

The most important here is the consideration of the case of pole approximation, as it represents the differential realization of decay widths. This allows the event generation within a cascade approach. However, the comparison with the complete calculations at the level of differential event distributions would be also required. That is the goal of a future work.

Acknowledgements. We are grateful to A. Arbuzov and L. Rumyantsev for discussions.

This work is partly supported by RFFI grant No. 07-02-00932-a; one of us (VK) thanks the grant «Dinastia»-2008.

REFERENCES

1. *Andonov A. et al.* // Comp. Phys. Commun. 2006. V. 174. P. 481.
2. *Bardin D. et al.* // Comp. Phys. Commun. 2007. V. 177. P. 738.
3. *Arbuzov A. et al.* // Eur. Phys. J. C. 2007. V. 51. P. 585.
4. *Sadykov R. et al.* // PoS. 2006. TOP2006. P. 036.
5. *Andonov A. et al.* // Part. Nucl., Lett. 2007. V. 4. P. 451.
6. *Vermaseren J. A. M.* math-ph/0010025.
7. *Andonov A. et al.* physics.comp-ph/0812.4207; CPC (submitted).
8. *Kolesnikov V. et al.* // PoS. 2008. ACAT08. P. 110.
9. Dubna: http://sanc.jinr.ru
   CERN: http://pcphsanc.cern.ch. 2007.
10. QCD–EW Corrections Interplay in Drell–Jan Like Single W- and Z-Production at LHC. *Sadykov R.* Part I: General Introduction, One-Loop Corrections in SANC; *Kolesnikov V.* Part II: NLO–QCD Corrections and Their Comparison with EW. Talks at ATLAS MC Working Group at CERN, Dec. 14, 2006; http://indico.cern.ch/conferenceDisplay.py? confId= 6818. 2006
11. *Andonov A. et al.* hep-ph/0901.2785; Phys. At. Nucl. 2010 (accepted).
12. *Passarino G., Veltman M. J. G.* // Nucl. Phys. B. 1979. V. 160. P. 151.
13. *Bardin D. Y., Passarino G.* The Standard Model in the Making: Precision Study of the Electroweak Interactions. Oxford, 1999. 685p.
14. *Bardin D., Kalinovskaya L., Rumyantsev L.* // Part. Nucl., Lett. 2009. V. 6, No. 1(150). P. 54.
15. *Wackeroth D., Hollik W.* // Phys. Rev. D. 1997. V. 55. P. 6788.
16. *Bardin D., Kalinovskaya L., Kolesnikov V.* // $J_{AW,WA}$ Functions for Processes of Single Top Production and Decay. In preparation.
17. *Yao W.-M. et al.* // J. Phys. G. 2006. V. 33. PDG.

Received on June 24, 2009.